

# Predicted Inversion Curve and Third Virial Coefficients of Carbon Dioxide at High Temperatures<sup>†</sup>

Coray M. Colina\* and Claudio Olivera-Fuentes

Department of Thermodynamics and Transport Phenomena, Simón Bolívar University, Caracas 1080, Venezuela

The shape of the Joule–Thomson inversion curve of a fluid at high temperatures is shown to be directly related to its second and third virial coefficients. Experimental values and empirical correlations of the third virial coefficient of carbon dioxide are used to resolve a previously observed conflict between inversion curves obtained from different equations of state for this fluid. In particular, third virial coefficients predicted from the Pitzer–Sterners equation of state are shown to be in error, resulting therefore in an incorrect inversion curve.

## Introduction

Recently, Chacín et al.<sup>1</sup> have presented molecular simulation results for the Joule–Thomson inversion curve of carbon dioxide. In the course of validating their results by comparison with experimental data and predictions from several equations of state (EOS), the authors observed an anomalous behavior of the inversion curve in the high temperature range. Here, the molecularly simulated curve deviated from the expected quasi-parabolic shape, exhibiting a change of slope and curvature (a “hump”) that ran contrary to the predictions of the Peng–Robinson<sup>2</sup> and Span–Wagner<sup>3</sup> EOS, yet appeared to be consistent with the experimental data of Price<sup>4</sup> and the predictions of the Pitzer–Sterners<sup>5</sup> EOS. Since both simulations and predictions carry their greatest uncertainty at the higher temperatures, the authors were unable to reach a clear conclusion regarding the accuracy of their molecular calculations near the maximum inversion temperature.

In the present work, we argue that the ability of an EOS to predict successfully the high temperature branch of the inversion curve is directly related to the quality of representation of the third virial coefficient. We compare third virial coefficients of carbon dioxide predicted by four multiparameter EOS with available experimental data and values generated from three empirical correlations. This analysis clearly demonstrates that the predictions of the Pitzer–Sterners<sup>5</sup> EOS at high temperatures are incorrect, and as a consequence the corresponding inversion curve cannot be accepted.

## Virial Coefficients and Inversion Curves

The Joule–Thomson inversion curve is the locus of thermodynamic states in which the temperature of a fluid does not change upon isenthalpic expansion

$$\left(\frac{\partial T}{\partial P}\right)_h = 0 \quad (1)$$

\* To whom correspondence should be addressed. Current address: Department of Chemical Engineering, North Carolina State University, Raleigh, NC 27695. Telephone: (919) 513-2051. Fax: (919) 513-2470. E-mail: ccolina@eos.ncsu.edu.

<sup>†</sup> In memory of Hasan Orbey, whom I was proud to call my friend (C.O.-F.).

The inversion criterion, eq 1, may be written in several alternative forms, e.g., for use with pressure-explicit EOS  $P = P(T, \rho)$

$$T \left( \frac{\partial P}{\partial T} \right)_\rho - \rho \left( \frac{\partial P}{\partial \rho} \right)_T = 0 \quad (2)$$

or for use with corresponding states models  $Z = Z(T_r, P_r)$

$$\left( \frac{\partial Z}{\partial T_r} \right)_{P_r} = 0 \quad (3)$$

Consider in particular the pressure-explicit (Leiden) form of the virial series

$$P = RT\rho(1 + B\rho + C\rho^2 + \dots) \quad (4)$$

Application of eq 2 yields the inversion condition

$$RT\rho \left[ \left( T \frac{dB}{dT} - B \right) \rho + \left( T \frac{dC}{dT} - 2C \right) \rho^2 + \dots \right] = 0 \quad (5)$$

In the high temperature region, where inversion pressures and densities go to zero as the fluid approaches ideal gas behavior, the virial series may be truncated at a conveniently small number of terms. Truncation after the third virial coefficient yields the simplest expression for the inversion density as a function of temperature

$$\rho_{\text{inv}} = - \frac{T(dB/dT) - B}{T(dC/dT) - 2C} = - \frac{1}{T} \frac{d(B/T)/dT}{d(C/T^2)/dT} \quad (6)$$

Thus, the second virial coefficient determines only the maximum inversion temperature corresponding to the limit of zero density, where the numerator of eq 6 vanishes. At low but finite densities, the inversion curve is governed by a combined function of  $B$  and  $C$ . It follows that any EOS that fails to predict third virial coefficients accurately will yield a correspondingly inaccurate inversion curve, at least at the higher temperatures. Even if second virial coefficients are well represented and the predicted curve terminates at the correct endpoint, it will approach this point from an incorrect direction, i.e., with the wrong slope and, possibly, curvature.

The range of validity of eq 6 is illustrated in Figure 1, which shows the complete inversion curve predicted

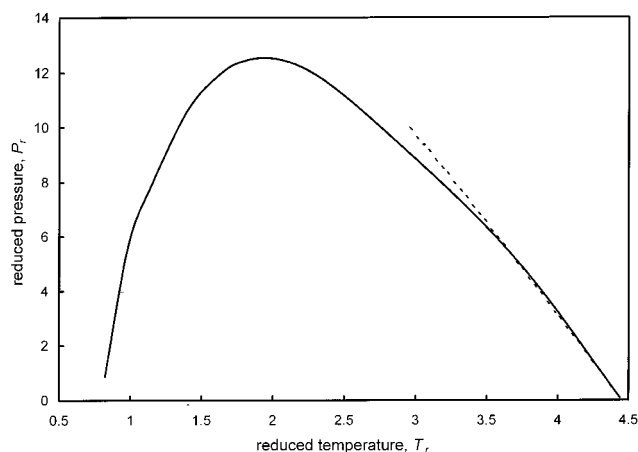


**Figure 1.** Inversion curve of carbon dioxide predicted by the Span-Wagner EOS. Dotted line is the virial approximation according to eqs 4 and 6.

for carbon dioxide using the Span-Wagner<sup>3</sup> EOS, and the upper temperature branch obtained by truncated virial expansion of the same EOS. Pressure differences at above 3 times the critical temperature ( $T > 900$  K) are less than 12%, and become progressively smaller as temperature increases. In this region, therefore, any doubts regarding a predicted inversion curve may be resolved by inspecting the third virial coefficients obtained from the same model.

### Third Virial Coefficients: Experimental Data and Correlations

Experimental values of third virial coefficients are considerably scarcer and less accurate than data on second virial coefficients. Values reported for carbon dioxide in the classic compilation of Dymond and Smith<sup>6</sup> come from six different sources and cover the temperature range from 262 to 773 K. Levelt Sengers et al.<sup>7</sup> give additional data between 273 and 420 K although these appear to be computed or smoothed values rather than derived from actual experimental measurements. More recent data by Holste et al.,<sup>8</sup> McElroy et al.,<sup>9</sup> and Duschek et al.<sup>10</sup> span essentially the same temperature range, 230–450 K.

Several corresponding-states correlations have been developed for the third virial coefficients of nonpolar gases (a condition not necessarily met by carbon dioxide, which becomes polar at high temperatures, but as will be seen below the correlations do represent the data for this fluid reasonably well in the region of interest). Chueh and Prausnitz<sup>11</sup> proposed a generalized function of the form

$$C\rho_c^2 = \mathcal{F}^{(0)}\{T_r\} + d\mathcal{F}^{(1)}\{T_r\} \quad (7)$$

but did not relate the empirical parameter  $d$  to fundamental pure fluid properties. De Santis and Grande<sup>12</sup> extended eq 7 to read

$$C\rho_c^2 = \mathcal{F}^{(0)}\{T_r\} + d\mathcal{F}^{(1)}\{T_r\} + d^2\mathcal{F}^{(2)}\{T_r\} \quad (8)$$

and suggested that the third parameter  $d$  be evaluated as

$$d = \frac{\omega\alpha N_0}{b} \quad (9)$$

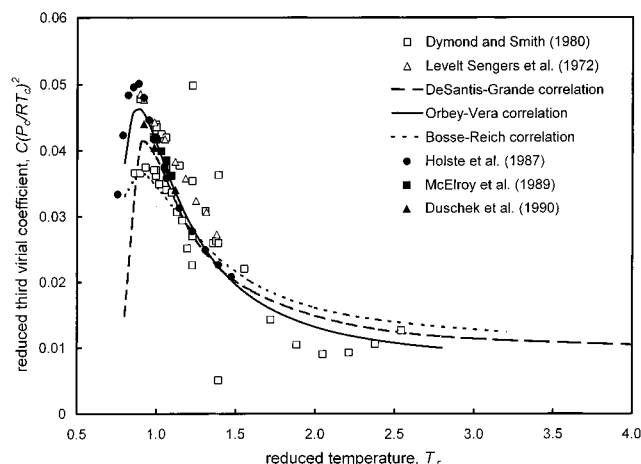


**Figure 2.** Experimental data on third virial coefficients of carbon dioxide and prediction from generalized correlations.

As shown by these authors, eq 8 is applicable over a wide range of reduced temperatures ( $0.8 < T_r < 4.0$ ). The contribution of the second and third terms is important only for  $T_r < 2.0$ , consistent with experimental findings.

Orbey and Vera<sup>13</sup> pointed out the practical convenience of employing acentric factor and critical temperature and pressure (rather than volume) as parameters in third virial coefficient correlations, since this is typically the information also required to estimate second virial coefficients of normal fluids. Their proposed correlation has the form

$$C\left(\frac{P_c}{RT_c}\right)^2 = \mathcal{F}^{(0)}\{T_r\} + \omega\mathcal{F}^{(1)}\{T_r\} \quad (10)$$

Limits of application for eq 10 were not given explicitly, but can be estimated from the context of their paper to be  $0 < \omega < 0.4$  and  $0.8 < T_r < 2.8$ .

Bosse and Reich<sup>14</sup> argued that the characteristic parameters used in the above correlations do not allow a clear separation of the different contributions to the third virial coefficient, such as pairwise additivity/nonadditivity and size/shape effects. They proposed instead a generalized dependence of the form

$$C\left(\frac{P_c}{RT_c}\right)^2 = \mathcal{F}^{(0)}\{T_r\} + \alpha^*\mathcal{F}^{(1)}\{T_r\} + (R_T^2 + R_T)\mathcal{F}^{(2)}\{T_r\} \quad (11)$$

where  $\alpha^*$  is the reduced dipolar polarizability defined as

$$\alpha^* \equiv \frac{P_c N_0}{RT_c} \alpha \quad (12)$$

Although these authors did not give limits for the application of eq 11, and carried out all comparisons in tabular rather than graphical form, all the experimental data used in their study lie in the interval  $0.80 < T_r < 3.18$ .

Figure 2 shows reduced third virial coefficients  $C_r$  for carbon dioxide. Experimental data are compared with predictions from eqs 8, 10, and 11. Discrepancies among these correlations are evident, but may simply reflect the use of different data subsets by each group of researchers. Figure 2 indicates that eqs 8 and 10

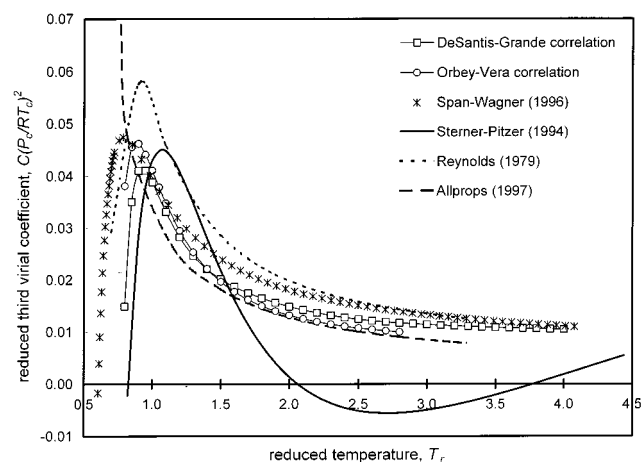


**Figure 3.** Equation of state prediction of third virial coefficients of carbon dioxide and comparison with generalized correlations.

perform better near the critical temperature, where eq 11 appears to underpredict the maximum value of  $C_r$ . In particular, eq 10 comes closest to the more recent data published after these correlations were developed. All three correlations predict a leveling out of the third virial coefficient at high temperatures, with eq 10 giving what is probably the lower bound. These are tentative conclusions in view of the high degree of scatter of the data, but are supported by similar studies for other fluids.<sup>15</sup> In general, it can be said that these correlations represent the available data within their experimental uncertainty, at least at the higher temperatures, and we will use eqs 8 and 10 instead of the original data to test the predictions of various EOS for carbon dioxide.

### Third Virial Coefficients: Prediction from Equations of State

Four EOS developed specifically for carbon dioxide are used here. These are the Bender<sup>16</sup> equation as reported by Reynolds,<sup>17</sup> the equations by Pitzer and Sterner<sup>5</sup> and by Span and Wagner<sup>3</sup> already mentioned, and the Ely et al.<sup>18</sup> equation implemented in the ALLPROPS computer package (Lemmon et al.<sup>19</sup>). Predicted third virial coefficients are shown in Figure 3 together with values generated from the DeSantis–Grande and Orbey–Vera correlations. It is immediately obvious from this comparison that the third virial coefficients predicted by the Pitzer–Sterner EOS are incorrect at high temperatures, becoming negative at about twice the critical temperature, reaching a minimum, and increasing again toward positive values at higher temperatures. These anomalous predictions will affect the corresponding inversion curve in two ways: first, an erroneous inversion density will be obtained, because of the incorrect value and sign of the derivative in the denominator of eq 6; and second, this error will be compounded on substituting the density back into eq 4 to obtain the inversion pressure, because of the incorrect value and sign of the third virial term.

Of the other three EOS included in Figure 3, the Ely et al. (ALLPROPS) equation fails to predict a maximum value of the virial coefficient at near critical temperatures, and possibly underpredicts it at higher temperatures. The Bender (Reynolds) equation does predict a maximum, although this is probably too high. At high temperatures, it comes into substantial agreement with the Span–Wagner equation, which appears very reliable

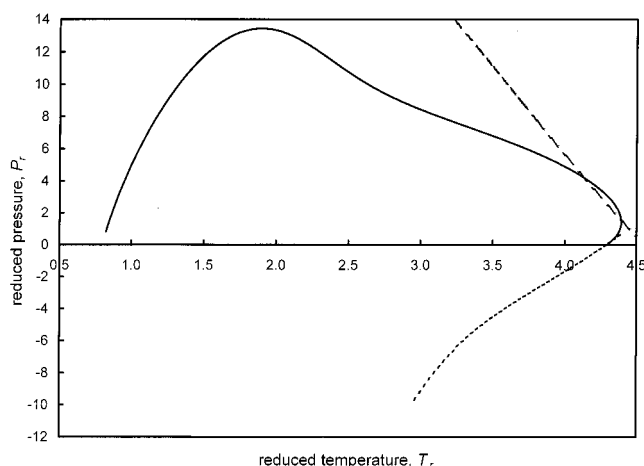


**Figure 4.** Inversion curve of carbon dioxide predicted by the Pitzer–Sterner EOS. Dotted line is the virial approximation using virial coefficients from the same EOS. Dashed line is the virial approximation using virial coefficients from generalized correlations.

over the entire temperature range. The two generalized correlations are confirmed to provide reasonable values, with the Orbey–Vera correlation being slightly preferable at lower temperatures.

Finally, we reinforce the above analysis by presenting in Figure 4 the inversion curve of carbon dioxide predicted by the Pitzer–Sterner EOS and comparing this at high temperatures with two virial approximations in terms of eqs 4 and 6. One of these, shown as a dashed line, has been obtained by combining the Orbey–Vera correlation for the third virial coefficient with the Tsonopoulos<sup>20</sup> correlation of second virial coefficients. The other, presented as a dotted line, is the virial approximation obtained from the EOS itself according to eqs 4 and 6. It is remarkable that the latter line approaches the inversion endpoint from negative pressure values, reflecting the errors in the third virial coefficient, as explained above. As a consequence, the Pitzer–Sterner inversion curve reaches its maximum inversion temperature at a positive pressure, and then bends back to the correct limiting value according to eq 6. This conduct is in strong disagreement with the expected shape of inversion curves as described by Deiters and De Reuck,<sup>21–23</sup> who state that “the Joule–Thomson inversion curve ... passes through one maximum ... and should have no further extrema or inflection points.” In an extensive comparative study of the extrapolation behavior of empirical equations of state, Span and Wagner<sup>24</sup> observed this deformation of the Joule–Thomson inversion curve predicted by the Sterner–Pitzer EOS and attributed it to “inconsistencies between the second virial coefficients and other data in the high-temperature region.” Cross-checking with Figure 3 shows that the anomalous “hump” or “overhang” of the curve starts to develop at the same temperature (about 2.5 times the critical temperature) at which the predicted third virial coefficient reaches a minimum and its temperature derivative becomes positive. There seems little doubt, therefore, that faulty representation of the third virial coefficient is responsible for this abnormal geometry of the inversion curve.

In light of the preceding discussion, it is inevitable to conclude that, although the Pitzer–Sterner inversion curve appears to approach a valid maximum inversion temperature, the shape of the end portion of this curve



(at reduced temperatures above 2.5) is incorrect. The molecular simulation results obtained by Chacín et al.<sup>1</sup> for carbon dioxide at high temperatures, which were mainly justified in terms of their agreement with this EOS, may therefore need to be regarded with some caution.<sup>25</sup>

## Conclusion

The prediction of second virial coefficients and their comparison with experimental values is a well-established, even mandatory test in the development of any EOS. By contrast, a similar verification of third virial coefficients is much less common, partly because the experimental data are less widely available, but also because their more complex dependence on temperature makes them intrinsically more difficult to represent by analytical models. However, good prediction of  $B$  alone is not sufficient to guarantee the correct behavior of an EOS, even at low or moderate densities. For instance, Chirico and Steele<sup>26</sup> have demonstrated the importance of the third virial coefficient in reconciling calorimetrically and spectroscopically derived entropies for benzene and methylbenzene at reduced temperatures  $T_r > 0.65$ . In the present work, we have shown by a simple analysis that third virial coefficients are also instrumental in predicting a correctly shaped inversion curve in the vicinity of the upper inversion temperature.

There is good reason, therefore, to suggest that an analysis of third virial coefficients should be performed as a routine test of any newly developed EOS. If experimental data are not available for comparison, the present study suggests that generalized correlations, e.g., that by Orbey and Vera,<sup>13</sup> may be relied on to supply the values needed to carry out such evaluations.

## Acknowledgment

The authors are grateful to Dr W. Wagner for making available the computational code for the Span–Wagner equation of state for carbon dioxide, in the revision programmed by the Lehrstuhl für Thermodynamik, Ruhr-Universität Bochum.

## Nomenclature

$b$  = Bondi molecular volume  
 $B$  = second virial coefficient  
 $C$  = third virial coefficient  
 $d$  = empirical parameter in generalized correlation; see eq 9  
 $\mathcal{F}$  = temperature function in generalized correlation  
 $h$  = enthalpy  
 $N_0$  = Avogadro's number  
 $P$  = pressure  
 $R$  = universal gas constant  
 $R_T$  = Thompson mean radius of gyration  
 $T$  = temperature  
 $Z$  = compressibility factor  
**Greek Symbols**  
 $\alpha$  = dipole polarizability  
 $\alpha^*$  = dimensionless dipole polarizability; see eq 12  
 $\omega$  = acentric factor  
 $\rho$  = density  
**Subscripts**  
 $c$  = critical property  
 $inv$  = inversion point  
 $r$  = reduced, relative to critical value

## Literature Cited

- Chacín, A.; Vázquez, J. M.; Müller, E. A. Molecular Simulation of the Joule-Thomson Inversion Curve of Carbon Dioxide. *Fluid Phase Equilib.* **1999**, *165*, 147.
- Peng, D.-Y.; Robinson, D. B. A New Two-Constant Equation of State. *Ind. Eng. Chem. Fundam.* **1976**, *15* (1), 59.
- Span, R.; Wagner, W. A New Equation of State for Carbon Dioxide Covering the Fluid Region from the Triple-Point Temperature to 1100 K at Pressures up to 800 MPa. *J. Phys. Chem. Ref. Data* **1996**, *25* (6), 1509.
- Price, D. Thermodynamic Functions of Carbon Dioxide—Joule-Thomson Coefficient, Isochoric Heat Capacity, and Isentropic Behavior at 100 to 1000° and 50 to 1400 Bars. *Ind. Eng. Chem., Chem. Eng. Data Ser.* **1956**, *1* (1), 83.
- Pitzer, K. S.; Sterner, S. M. Equations of State Valid Continuously from Zero to Extreme Pressures for H<sub>2</sub>O and CO<sub>2</sub>. *J. Chem. Phys.* **1994**, *101* (4), 3111.
- Dymond, J. H.; Smith, D. B. *The Virial Coefficients of Gases. A Critical Compilation*; Clarendon Press: Oxford, 1980.
- Levelt Sengers, J. M. H.; Klein, M.; Gallagher, J. S. Pressure—Volume—Temperature Relationships of Gases. In *American Institute of Physics Handbook*, 3rd ed.; Gray, D. E., Ed.; McGraw-Hill: New York, 1972; Virial Coefficients, Section 4i.
- Holste, J. C.; Hall, K. R.; Eubank, P. T.; Esper, G.; Watson, M. Q.; Warowny, W.; Bailey, D. M.; Young, J. G.; Bellomy, M. T. Experimental ( $p$ ,  $V_m$ ,  $T$ ) for Pure Carbon Dioxide Between 220 and 450 K. *J. Chem. Thermodyn.* **1987**, *19* (12), 1233.
- McElroy, P. J.; Battino, R.; Dowd, M. K. Compression-Factor Measurements on Methane, Carbon Dioxide, and (Methane + Carbon Dioxide) Using a Weighing Method. *J. Chem. Thermodyn.* **1989**, *21* (12), 1287.
- Duschek, W.; Kleinrahm, R.; Wagner, W. Measurement and Correlation of the (Pressure, Density, Temperature) Relation of Carbon Dioxide. I. The Homogeneous Gas and Liquid Regions in the Temperature Range from 217 K to 340 K at Pressures up to 9 MPa. *J. Chem. Thermodyn.* **1990**, *22* (9), 827.
- Chueh, P. L.; Prausnitz, J. M. Third Virial Coefficients of NonPolar Gases and their Mixtures. *AIChE J.* **1967**, *13* (5), 896.
- De Santis, R.; Grande, B. An Equation for Predicting Third Virial Coefficients of Nonpolar Gases. *AIChE J.* **1979**, *25* (6), 931.
- Orbey, H.; Vera, J. H. Correlation for the Third Virial Coefficient Using  $T_c$ ,  $P_c$  and  $\omega$  as Parameters. *AIChE J.* **1983**, *29* (1), 107.
- Bosse, M. A.; Reich, R. Correlation for the Third Virial Coefficient Using  $T_c$ ,  $P_c$ , Dipolar Polarizability and Mean Radius of Gyration as Parameters. *Chem. Eng. Commun.* **1988**, *66*, 83.
- Colina, C. M.; Olivera-Fuentes, C. Evaluation of Equations of State through Third Virial Coefficients. Presented at the Fifth IberoAmerican Conference on Fluid Properties and Phase Equilibria for Chemical Process Design (Equifase 99): Vigo, Spain, 1999.
- Bender, E. Equations of State Exactly Representing the Phase Behavior of Pure Substances. *Proceedings of the 5th Symposium on Thermophysical Properties*; ASME: 1970; p 227.
- Reynolds, W. C. *Thermodynamic Properties in SI*; Department of Mechanical Engineering, Stanford University: Stanford, CA, 1979.
- Ely, J. F.; Magee, J. W.; Haynes, W. M. *Thermophysical Properties for Special High CO<sub>2</sub> Content Mixtures*; Research Report 110; Gas Processors Association, 1987.
- Lemmon, E. W.; Jacobsen, R. T.; Penoncello, S. G.; Beyrerlein, S. W. *Computer Programs for Calculating Thermodynamic Properties of Fluids of Engineering Interest*; Report 97-1; Center for Applied Thermodynamic Studies, University of Idaho: Moscow, ID, 1997.
- Tsonopoulos, C. An Empirical Correlation of Second Virial Coefficients. *AIChE J.* **1974**, *20* (2), 263.
- Deiters, U.; De Reuck, K. M. Guidelines for Publication of Equations of State-I. Pure Fluids. Technical Report. *Pure Appl. Chem.* **1997**, *69*, 1237.
- Deiters, U. K.; De Reuck, K. M. Guidelines for Publication of Equations of State-I. Pure fluids. *Chem. Eng. J.* **1998**, *69*, 69.
- Deiters, U. K. Remarks on publications dealing with equations of state. *Fluid Phase Equilib.* **1999**, *161*, 205.

(24) Span, R.; Wagner, W. On the Extrapolation Behavior of Empirical Equations of State. *Int. J. Thermophys.* **1997**, *18*, 1415.

(25) Escobedo, F. A.; Chen, Z. Simulation of Isoenthalps and Joule-Thomson Inversion Curves for Pure Fluids and Mixtures. *Mol. Simul.* **2001**, *26*, 395.

(26) Chirico, R. D.; Steel, W. M. Reconciliation of Calorimetrically and Spectroscopically Derived Thermodynamic Properties at Pressures Greater Than 0.1 MPa for Benzene and Meth-

ylbenzene: The Importance of the Third Virial Coefficient. *Ind. Eng. Chem. Res.* **1994**, *33*, 157.

*Received for review April 25, 2001*

*Revised manuscript received August 31, 2001*

*Accepted September 5, 2001*

IE010367S